archives
of thermodynamics
Vol. **43**(2022), No. 4, 109–133
DOI: 10.24425/ather.2022.144408

Thermodynamic assessment of thermochemical cycle for hydrogen production based on water decomposition with binary copper chlorine couple

OMAR BENBRIKA[a]
AHMED BENSENOUCI[a*]
MOHAMED TEGAR[a]
KAMAL R.A. ISMAIL[b]

[a] Laboratory of Mechanics, Amar Telidji University of Laghouat, B.P. 37G Laghouat 03000, Algeria

[b] University of Campinas, Sao Paulo 13083-970, Brazil

Abstract The present study aims at investigating and simulating the hydrogen cycle production at low temperatures using thermochemical reactions. The cycle used in this work is based on the dissociation of water molecules depending on a copper chlorine couple. Furthermore, the proposed method uses mainly thermal energy provided by a solar thermal field. This proposed cycle differs from what is found in the literature. However, most of the thermochemical cycles for hydrogen production work at quite high temperatures which is a technical challenge. Therefore, the maximum temperature used in the present cycle is limited to 500°C. A thermodynamic analysis based on both the first and second laws is performed to evaluate the energy, exergy and efficiency of each reaction as well as the overall exergetic efficiency of the system. Furthermore, a parametric study is conducted to figure out the impact of the surrounding temperatures on the overall exergetic efficiency using commercial energy simulation software. The results show that the cycle can achieve an exergy efficiency of 30.5%.

Keywords: Hydrogen production; Thermochemical process; Copper-chlorine cycle; Water dissociate; Exergy and energy analyses

*Corresponding Author. Email: a.bensenouci@lagh-univ.dz

Nomenclature

Ex	–	exergy, KJ
$\overline{ex}$	–	specific exergy, kJ/mol
$\overline{ex}^{ph}$	–	specific physical exergy, kJ/mol
$\overline{ex}^{ch}$	–	specific chemical exergy, kJ/mol
G	–	Gibbs function, kJ
g_f^0	–	specific Gibbs free energy of formation, KJ/Kmol
g	–	gravity, m/s^2
H	–	enthalpy, kJ
$\dot{H}$	–	total enthalpy, kJ
$\overline{h}_f^0$	–	specific molar enthalpy of formation, kJ/Kmol
$\overline{h}$	–	molar enthalpy, kJ/mol
$\overline{h}^0$	–	sensible molar enthalpy at standards conditions, kJ/mol
$\dot{m}$	–	mass flow rate, kg/s
n	–	mole number, kmol
n_R	–	number of moles of reactants, kmol
n_P	–	number of moles of products, kmol
P	–	pressure, bar
P_0	–	reference pressure, atm
$\dot{Q}$	–	heat transfer, kJ
R	–	ideal gas constant, kJ/kmol.K
S	–	entropy, kJ/K
$\overline{s}$	–	molar entropy, kJ/kmol.K
$\overline{s}^0$	–	standard specific entropy, J/mol.K
T	–	temperature, °C
T_0	–	environment temperature, °C
T_{rea}	–	reaction temperature, °C
V	–	speed, m/s
W	–	work, kJ
z	–	height, m
(g)	–	gas
(l)	–	liquid
(s)	–	solid

Greek symbols

η_{ex}	–	exergy efficiency
$\eta_{ex\,\text{overall}}$	–	overall exergy efficiency
$\eta_{R1},\ \eta_{R2},\ \eta_{R3}$	–	exergetic efficiency of different stages

Acronyms

EES	–	Engineering Equation Solver
GHG	–	greenhouse gas
TWSCs	–	thermochemical water splitting cycles
SMR	–	steam methane reforming

Subscripts

in	–	input
dest	–	destruction
f	–	formation
out	–	output
P	–	product
R	–	reactant

1 Introduction

Global energy demand is continuously increasing mainly due to increasing population and economic growth. Currently, fossil fuels provide 80% of the world's primary energy [1] and this causes serious environmental problems and global warming. As a result, tremendous efforts are globally done to use renewable energy for sustainability purposes. Therefore, hydrogen has emerged as a compelling answer to these challenges [2]. It is expected that hydrogen will be the main energy of the next generation because of its features, including sustainability, environmental friendly, dispatchable, and abundant [3]. In addition, hydrogen is considered the main string among consuming industries such as ethanol and ammonia production plants as well as other important sectors, including gas grid, agriculture, electricity grid, residential, energy storage and transportation [4, 5]. In a prospective study, it was shown that hydrogen can meet 18% of the world's energy consumption (equivalent to 78 EJ) in 2050 [6]. To make the hydrogen economy a practical choice, a fundamental issue concerning hydrogen production must be solved [7]. Hydrogen production can be done in various ways. It is generally produced using the steam methane reforming (SMR) process, which produces methane exhaust and leads to high greenhouse gas emissions (GHG). Nearly half of the world's hydrogen demand is satisfied by SMR, with around 30% of hydrogen generated by oil reforming, 18% by coal gasification, and nearly 4% by water electrolysis [6, 8], while renewable sources of hydrogen production account for less than 1% of the total hydrogen production [6, 9]. Despite the significant progress in the hydrogen economy over the last few decades, numerous problems remain unsolved including the shortage of hydrogen in its unadulterated structure at the climate, the intricacy of purification and production, cost and significant expense, and the storage capacity. The sustainable energy and hydrogen economy can be improved by increasing hydrogen creation innovations, for

example thermochemical water-splitting cycles (TWSCs) in a sustainable and integrated way for extensive hydrogen generation.

The thermochemical water-splitting cycles are among the most environmentally friendly techniques to produce pure hydrogen using heat from renewable and clean sources. The most important energy sources usually involved in this cycle to break down the water molecule into oxygen and hydrogen gas molecules are solar energy [10–13], nuclear energy [14, 15], biomass energy [16], geothermal energy [17] as well as a combination of resources of these energies, like concentrated solar energy and geothermal energy [18]. Adding an electrochemical reaction technique inside the cycle is also employed to reduce the reaction temperature [19]. In this process, several chemical reactions occur where only water and heat are supplied and all chemical reactants are regenerated and recycled inside the system without emitting any pollutants into the environment [20].

Numerous investigations and reviews have been presented in the last four decades where various thermochemical cycles have been offered for the production of hydrogen [21]. About 280 hydrogen production processes utilizing thermochemical cycles have been discovered. However, a few showed promising results [22]. After considering different issues like the abundance of materials, thermodynamic feasibility, chemical viability, simplicity and safety issues, the following eight cycles were considered promising cycles: magnesium chloride (Mg–Cl) [2, 23], iron chlorine (Fe–Cl) [24], magnesium iodide (Mg–I) [25], vanadium chlorine (V–Cl) [26], cerium chlorine (Ce–Cl) [27], hybrid chlorine [28], the sulfuric acid (H_2SO_4) [29], copper chlorine (Cu–Cl) [30–32]. The vast majority of these cycles need a heat source to work properly at temperatures higher than 800°C. While, the Cu Cl cycle has several advantages over other cycles because of its relatively lower temperature (about 550°C) [33], as well as low maintenance costs and reduced material. Moreover, waste heat can be utilized increasing thus the system efficiency [34, 35].

In this paper, a new cycle is studied thermodynamically. The proposed system is based on three chemical reactions. Analysis of energy and exergy enables assessment of the thermodynamic system. Different assessments are performed utilizing thermochemistry and thermodynamic tools [36]. A commercial software package, Engineering Equation Solver (EES) [37] software is used for simulations and thermodynamic modelling of the results. This research focuses on the proposed copper chlorine (Cu–Cl) cycle to show the strengths, shortcomings, and gaps to create new techniques for producing cost-effective hydrogen.

2 Description of the cycle

This cycle including copper and chlorine proposed in this study is different from what is found in the literature, where the decomposition of water is made by thermochemical means using heat as a driver to obtain oxygen and hydrogen. This cycle can have as a thermal source [38], solar energy, nuclear energy, heat recovered from thermal power stations, gas turbines and means of transport such as cars, buses, trucks, etc.

The cycle consists essentially of three stages, summarized in Table 1 and Fig. 1. The three stages require thermal energy. Research and developments concerning the reactions of this cycle are relatively mature. The process consists of a closed internal loop that continuously recycles all copper chlorine molecules. The principal reaction is that related to hydrogen production; the two remaining ones are used to recycle the chemical components for the continuity of the process. The symbols (g), (l), and (s) in the chemical formulae of the reaction stand for gas, liquid, and solid, respectively.

Table 1: Chemical reactions.

Step	Reaction	Temperature/Pressure (°C/atm)
Production of $Cu\backslash Cl_2$	$CuCl_2(s) \rightarrow Cu(s) + Cl_2(g)$	400–500
Production of $HCl\backslash O_2$	$Cl_2(g) + H_2O(l) + Q \rightarrow 2HCl(g) + 1/2O_2(g)$	350–400
Production of H_2	$Cu(s) + 2HCl(g) \rightarrow CuCl_2(s) + H_2(g) + Q$	< 50

(g) – gas, (l) – liquid, (s) – solid

The mechanism of this cycle is first started by a decomposition of Dichloro copper in solid state to produce gas chlorine and copper in solid state within a temperature range of 400−500°C, which is the highest of the cycle. In the second step, water and chlorine gas are used to obtain half a mole of oxygen and two moles of hydrochloric acid; both products are in gaseous state. The reverse Deacon reaction is the name given to this reaction. In the third reaction, Cu reacts with the hydrochloric acid HCl to form solid copper (II) chloride $CuCl_2$ to be reused in the first reaction in addition to one mole of hydrogen gas H_2; this reaction is exothermic. The Cu–Cl-based thermochemical cycle is one of the promising techniques for producing hydrogen at a temperature of 400−500°C and without releasing greenhouse gas emissions.

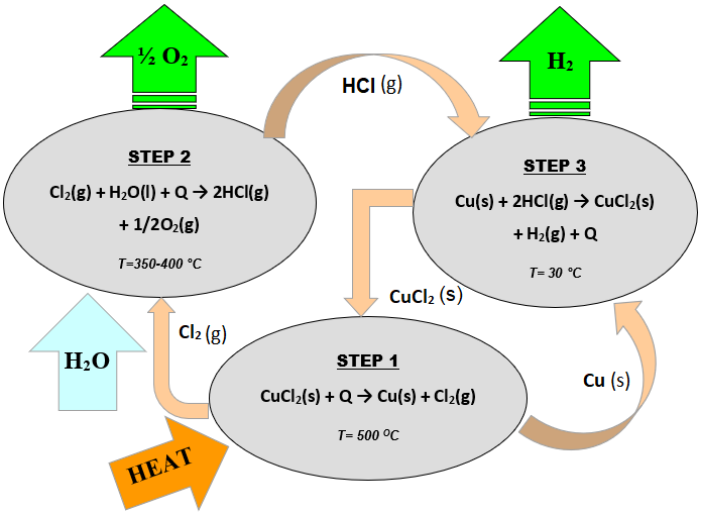

Figure 1: Diagram of the Cu–Cl thermochemical cycle; g – gas, l – liquid, s – solid.

3 Feasibility of chemical reactions

Before starting the analysis of this cycle, the three chemical equations are checked up to ensure that the reactions are feasible by finding the values of the Gibbs function. This function can predict the direction of the chemical reaction. It is the most useful criterion for predicting the direction of a chemical reaction and the composition of the system at an equilibrium state [39] which must be less than zero to be feasible and spontaneous. The Gibbs free energy, denoted G, combines enthalpy and entropy (combining the first law and second law of thermodynamics) into a single value. The change in free energy ΔG, is equal to the sum of the enthalpy change and the product of the temperature and entropy change of the system $\Delta G = \Delta H - T\Delta S$, where G is free enthalpy or Gibbs function and considered as a function of state, T is the temperature and S is the entropy, H is the enthalpy [40, 41].

At constant temperature and pressure, we note that:

- $\Delta G < 0$ – spontaneous reaction,
- $\Delta G = 0$ – the system is in balance,
- $\Delta G > 0$ – non-spontaneous reaction (not possible).

We have the following chemical reactions to check:

1. $CuCl_2(s) \rightarrow Cu(s) + Cl_2(g)$,
2. $Cl_2(g) + H_2O(l) \rightarrow HCl(g) + O_2(g)$,
3. $Cu(s) + HCl(g) \rightarrow CuCl_2(s) + H_2(g)$.

Application of the Gibbs function on the first reaction.
Reaction 1; $CuCl_2(s) \rightarrow Cu(s) + Cl_2(g)$

$$\Delta G_{\text{Reaction 1}} = \Delta G_{CuCl_2} - (\Delta G_{Cu} - \Delta G_{Cl_2}), \tag{1}$$

$$\begin{aligned} \Delta G_{CuCl_2} &= \Delta H_{CuCl_2} - T\Delta S_{CuCl_2} \quad \text{or} \\ \Delta G_{CuCl_2} &= \left(\overline{h} - \overline{h}^0\right)_{CuCl_2} - T\left(\overline{s} - \overline{s}^0\right)_{CuCl_2}, \end{aligned} \tag{2}$$

$$\begin{aligned} \Delta G_{\text{Reaction 1}} = &\left(\overline{h} - \overline{h}^0\right)_{CuCl_2} - T\left(\overline{s} - \overline{s}^0\right)_{CuCl_2} - \left(\overline{h} - \overline{h}^0\right)_{Cu} \\ &+ T\left(\overline{s} - \overline{s}^0\right)_{Cu} - \left(\overline{h} - \overline{h}^0\right)_{Cl_2} + T\left(\overline{s} - \overline{s}^0\right)_{Cl_2}. \end{aligned} \tag{3}$$

We use the Shomate equations to develop the specific molar entropy $(\overline{s} - \overline{s}^0)$ and specific molar enthalpy $(\overline{h} - \overline{h}^0)$ values. (The Shomate equations will be explained in Subsection 4.2). Using Eq. (1), with the help of EES software, we get the following curve of reaction 1 in Fig. 2. We follow the same steps to obtain the second and third curves of the chemical equations.

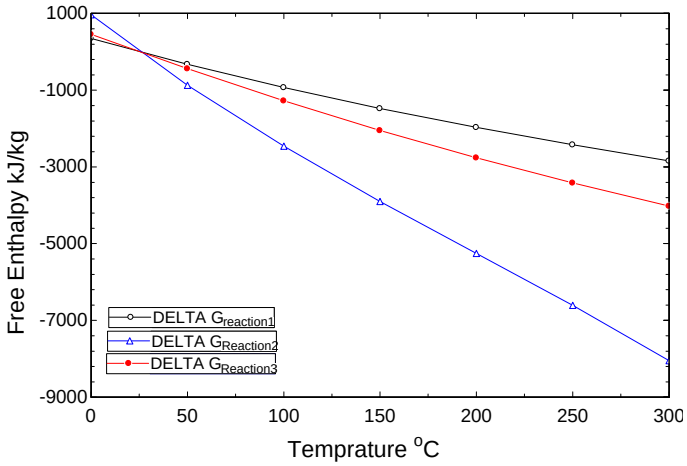

Figure 2: Variation of Gibbs function with temperature.

Figure 2 shows the change of free enthalpy with temperature. The results clearly illustrate that the three chemical reactions are all feasible because their Gibbs functions or free enthalpy is less than zero. One can observe that with the increase of the temperature the Gibbs function increases in the negative direction, which means all reactions are more profitable and spontaneous.

4 Analysis

4.1 Energy analysis

As a contribution to a sustainable plan to address the increasing energy requirements, the Cu–Cl cycle can be a viable candidate for the production of hydrogen for energy supply. The following quantities are given in terms of kilomole of hydrogen produced, where 1 kilomole of hydrogen is produced per cycle. In addition, the following assumptions are considered:

- ambient temperature (T_0), and pressure (P_0) of the surroundings are considered;
- the temperature of the reactants and products are at the chemical reaction temperature;
- steady-state with negligible kinetic energy and potential effects are assumed.

In the steady-state condition, the mass balance is expressed by the mass conservation law [42]

$$\sum \dot{m}_{\text{in}} = \sum \dot{m}_{\text{out}} \,, \tag{4}$$

where $\dot{m}$ represents the mass flow rate. The molar heat transfer can be extracted from the energy balance: $\dot{E}_{\text{in}} - \dot{E}_{\text{out}} = \Delta \dot{E}_{\text{sys}}$, where $\Delta \dot{E}_{\text{sys}}$ is the rate of energy change of the system. It is assumed that the chemical reactions are done without work, $W = 0$. With a steady state reaction, the energy balance can be written as

$$\dot{Q} = \dot{H}_P - \dot{H}_R = \sum n_P \left(\overline{h}_f^0 + \overline{h} - \overline{h}^0\right)_P - \sum n_R \left(\overline{h}_f^0 + \overline{h} - \overline{h}^0\right)_R . \tag{5}$$

4.2 Exergy analysis

For a process involving a chemical reaction, the exergy balance can be written as follows [43]:

$$Ex_{\text{in}} - Ex_{\text{out}} - Ex_{\text{dest}} = \Delta Ex_{\text{sys}}\,. \tag{6}$$

For a steady-state process, $\Delta \dot{E}x_{\text{sys}}$ is equal to zero. Therefore, the exergy destroyed is the difference between the exergies entering the system minus the exergies leaving the system, and the specific exergy of flow can be written as follows:

$$\overline{ex} = \overline{ex}^{\,ph} + \overline{ex}^{\,ch}, \tag{7}$$

with

$$\overline{ex}^{\,ph} = \left(\overline{h} - \overline{h}^{0}\right) - T_0\left(\overline{s} - \overline{s}^{0}\right) + \frac{V^2}{2} + gz, \tag{8}$$

where V is the speed, g is the gravitational acceleration and z is the height.

The specific kinetic energy ($V^2/2$) and specific potential energy (gz) terms of the physical exergies $\overline{ex}^{\,ph}$ are neglected in this analysis, $\overline{ex}^{\,ch}$ is the chemical exergy. Combining Eqs. (7) and (8), one can obtain the destroyed exergy:

$$\begin{aligned} Ex_{\text{dest}} = &\sum_{\text{in}} n\left[\left(\overline{h} - \overline{h}^{0}\right) - T_0\left(\overline{s} - \overline{s}^{0}\right) + \overline{ex}^{\,ch}\right]_{\text{in}} \\ &- \sum_{\text{out}} n\left[\left(\overline{h} - \overline{h}^{0}\right) - T_0\left(\overline{s} - \overline{s}^{0}\right) + \overline{ex}^{\,ch}\right]_{\text{out}} + \left(1 - \frac{T_0}{T_{\text{rea}}}\right)\dot{Q}, \end{aligned} \tag{9}$$

where n is the mole number, T_{rea} is the reaction temperature and $\dot{Q}$ is the heat flow into the system as given in Eq. (5) is positive for endothermic reaction and negative for exothermic one.

After the development of the mass balance and energy as well as exergy analysis of the cycle, the National Institute of Standards and Technology (NIST) database [44] is used to obtain the specific entropy ($\overline{s} - \overline{s}^{0}$) and enthalpy ($\overline{h} - \overline{h}^{0}$) values of all reactants through the Shomate equations

$$\overline{h} - \overline{h}^{0} = At + B\frac{t^2}{2} + C\frac{t^3}{3} + D\frac{t^4}{4} + E\frac{1}{t} + F - H \tag{10}$$

and

$$\overline{s} = A\ln t + Bt + C\frac{t^2}{2} + D\frac{t^3}{3} - E\frac{1}{2t^2} + G - R\ln\frac{P_{\text{rea}}}{P_0} \tag{11}$$

with $t = \dfrac{T}{1000}$, where R is the ideal gas constant, P_{rea} is pressure of reaction. The constants A, B, C, D, E, F, G, H are given in Table 2 for each chemical element involved in chemical interaction. T is the temperature specified in Kelvin. Values of the specific enthalpies and entropies are given in Table 3. From that, we calculate the value of the specific chemical exergy for each compound. Chemical exergy based on the value of typical reference exergy taken under standard conditions is called standard chemical exergy. To find the standard chemical exergy of an element not found in nature, one considers the interaction of this element with other compounds for which their standard chemical exergy is known:

$$\overline{ex}^{\,ch} = -\Delta G + \sum_{P} n\,\overline{ex}^{\,ch} - \sum_{R} n\,\overline{ex}^{\,ch}, \tag{12}$$

where ΔG is the variation of free enthalpy at the standard temperature T_0 and pressure P_0 of the reactants and products. The constant n expresses the

Table 2: Shomate constants for the compounds [45].

Compounds	A	B	C	D	E	F	G	H
$CuCl_2$(s)	70.21882	23.36132	–14.86876	4.053899	–0.366203	–228.9405	184.6378	–205.8532
Cu(s)	17.72891	28.0987	–31.25289	13.97243	0.068611	–6.056591	47.89592	0
Cl_2(g)	33.0506	12.2294	–12.0651	4.38533	–0.159494	–10.8348	259.029	0
H_2O(l)	–203.606	1523.29	–3196.413	2474.455	3.855326	–256.5478	–488.7163	–285.8304
HCl(g)	32.12392	–13.45805	19.86852	–6.85393	–0.049672	–101.6206	228.6866	–92.31201
O_2(g)	31.32234	–20.23531	57.86644	–36.5062	–0.007374	–8.903471	246.7945	0
H_2(g)	33.066178	–11.363417	11.432816	–2.77287	–0.158558	–9.980797	172.707974	0

Table 3: Specific standard entropy and enthalpy of the compounds of the chemical reaction [46].

Compounds	Enthalpy of specific standard formation $-\overline{h}_f^0$ (kJ/kmol)	Standard specific entropy $-\overline{s}^0$ (J/molK)
H_2(g)	0	130.68
Cu(s)	0	33.15
HCl(g)	–92 310	186.9
$CuCl_2$(s)	–205 850	108.06
Cl_2(s)	0	223.08
H_2O(l)	–285 830	69.95
O_2(g)	0	205.15

number of moles of the substances. In the present case, the chemical exergy of copper chloride $CuCl_2$ is obtained from the basic constituent elements of this molecule, for which the standard chemical exergy is already known. The formation reaction of this molecule is as follows:

$$Cu + Cl_2 \rightarrow CuCl_2\,.$$

One can write Eq. (13) as follows:

$$\overline{ex}^{ch}_{CuCl_2} = [g_{CuCl_2} - g_{Cu} - g_{Cl_2}]\,(T_0 P_0) = +\overline{ex}^{ch}_{Cu_2} + \overline{ex}^{ch}_{Cl2_2}\,. \tag{13}$$

The variation of the specific Gibbs function for this reaction is

$$g_P - g_R = (h - Ts)_{CuCl_2} - (h - Ts)_{Cu} - (h - Ts)_{Cl_2} \tag{14}$$

with

$$\begin{aligned} g_R &= g_{Cu} - g_{Cl_2} = 0 \quad \text{and} \\ g_P &= g^0_{fCuCl_2} = h^0_{fCuCl_2} - T_0\left(s^0_{CuCl_2} - s^0_{Cu} - s^0_{Cl_2}\right). \end{aligned} \tag{15}$$

We can write the chemical exergy of copper chloride as follows:

$$\overline{ex}^{ch}_{CuCl_2} = h^0_{fCuCl_2} - T_0\left(s^0_{CuCl_2} - s^0_{Cu} - s^0_{Cl_2}\right) + \overline{ex}^{ch}_{Cu_2} + \overline{ex}^{ch}_{Cl2_2}. \tag{16}$$

According to this procedure, one can obtain the other compounds of standard chemical exergy not found in nature. In addition, one can utilize the exergy balance for evaluating the exergy efficiency of each chemical reaction and have a complete view of the Cu–Cl cycle and calculate its efficiency. Under steady-state conditions, one can also neglect the exergy transfer to the external environment in the form of exergy losses.

Table 4: Standard chemical exergy and Gibbs free energy [46].

Compound	Specific Gibbs free energy of formation (kJ/kmol)	Specific standard chemical exergy $\overline{ex}^{ch}$ (kJ/mol)
$CuCl_2$(s)	–161 689	82.10
H_2O(l)	–237 170	0.92
HCl(g)	–95 296	84.73
Cu(s)	0	134.20
O_2(g)	0	3.97
H_2(g)	0	236.10
Cl_2(g)	0	123.60

Moreover, no work transfer is considered with the external environment, $W = 0$. One can evaluate the exergy efficiency by the following equation:

$$\eta_{ex} = \frac{\overline{ex}_{\text{out}}}{\overline{ex}_{\text{in}}}, \tag{17}$$

where $\overline{ex}_{\text{out}}$ is the exergy that exists in the system, $\overline{ex}_{\text{in}}$ is the exergy that enters the system. The exergy efficiency is then

$$\eta_{ex} = 1 - \frac{\overline{ex}_{\text{dest}}}{\overline{ex}_{\text{in}}}. \tag{18}$$

4.3 First reaction analysis

Figure 3 presents the decomposition of the solid copper bichloride ($CuCl_2$) to obtain copper (Cu) in the solid state and chlorine gas. Where the reaction temperature can achieve 550°C, the system is in a stable state and the transformation is adiabatic and endothermic.

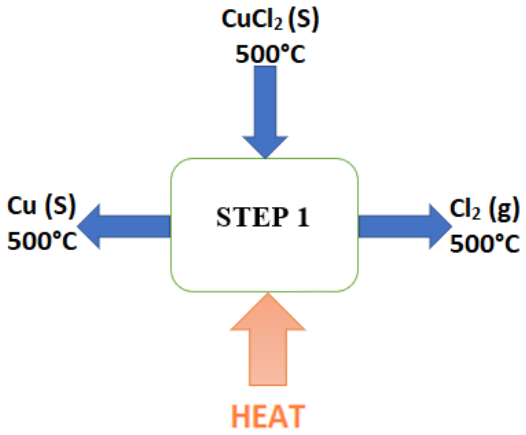

Figure 3: Step of Cu and Cl_2 production.

The heat transfer for the first reaction is determined as follows:

$$\dot{Q} = \left[n\left(\overline{h}_f^0 + \overline{h} - \overline{h}^0\right)\right]_{\text{Cu}} + \left[n_P\left(\overline{h}_f^0 + \overline{h} - \overline{h}^0\right)\right]_{\text{Cl}_2} - \left[n\left(\overline{h}_f^0 + \overline{h} - \overline{h}^0\right)\right]_{\text{CuCl}_2}. \tag{19}$$

The destroyed energy is written as

$$Ex_{\text{dest}} = \left[\left(\overline{h} - \overline{h}^{0}\right) - T_0\left(\overline{s} - \overline{s}^{0}\right) + \overline{ex}^{ch}\right]_{CuCl_2} - \left[\left(\overline{h} - \overline{h}^{0}\right) - T_0\left(\overline{s} - \overline{s}^{0}\right) + \overline{ex}^{ch}\right]_{Cu} - \left[\left(\overline{h} - \overline{h}^{0}\right) - T_0\left(\overline{s} - \overline{s}^{0}\right) + \overline{ex}^{ch}\right]_{Cl_2} + \left(1 - \frac{T_0}{T_{\text{rea}}}\right)\dot{Q}\,. \quad (20)$$

4.4 Second reaction analysis

In this step, the chlorine is heated with water until it produces oxygen (O_2) and hydrochloric acid (HCl) in gaseous state as shown in Fig. 4. The temperature of this reaction varies from 300°C to 450°C, the second reaction is considered an adiabatic transformation and endothermic in nature.

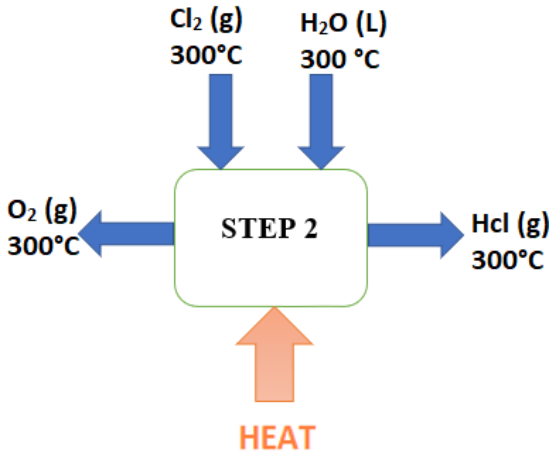

Figure 4: Step of HCl and O_2 production.

The molar heat transfer for the second step can be determined as follows:

$$\dot{Q} = \left[n\left(\overline{h}_f^0 + \overline{h} - \overline{h}^{0}\right)\right]_{HCl} + \left[n\left(\overline{h}_f^0 + \overline{h} - \overline{h}^{0}\right)\right]_{O_2} - \left[n\left(\overline{h}_f^0 + \overline{h} - \overline{h}^{0}\right)\right]_{Cl_2} - \left[n\left(\overline{h}_f^0 + \overline{h} - \overline{h}^{0}\right)\right]_{H_2O}\,. \quad (21)$$

The destroyed energy is written as

$$\begin{aligned} Ex_{\text{dest}} = &\left[\left(\overline{h}-\overline{h}^{0}\right)-T_0\left(\overline{s}-\overline{s}^{0}\right)+\overline{ex}^{ch}\right]_{Cl_2} \\ &+\left[\left(\overline{h}-\overline{h}^{0}\right)-T_0\left(\overline{s}-\overline{s}^{0}\right)+\overline{ex}^{ch}\right]_{H_2O} \\ &-\left[\left(\overline{h}-\overline{h}^{0}\right)-T_0\left(\overline{s}-\overline{s}^{0}\right)+\overline{ex}^{ch}\right]_{HCl} \\ &-\left[\left(\overline{h}-\overline{h}^{0}\right)-T_0\left(\overline{s}-\overline{s}^{0}\right)+\overline{ex}^{ch}\right]_{O_2}+\left(1-\frac{T_0}{T_{\text{rea}}}\right)\dot{Q}\,. \end{aligned} \tag{22}$$

4.5 Third reaction analysis

In the last step, both components copper (Cu) and hydrogen-chloride (HCl) react to be copper bichloride ($CuCl_2$) and the gas of hydrogen, like in Fig. 5. This interaction is below 50°C. The third reaction is considered an adiabatic transformation and exothermic in nature.

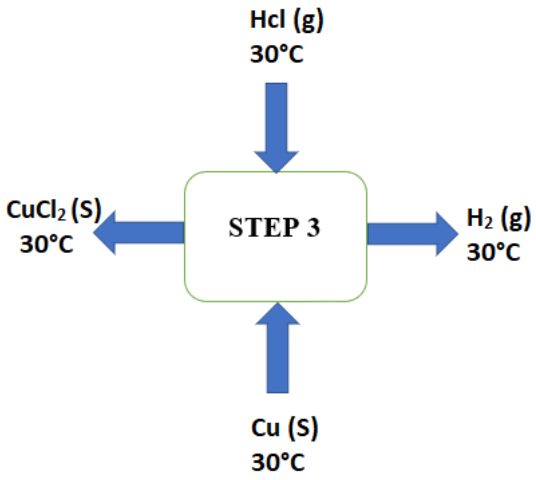

Figure 5: Step of H_2 production.

The molar heat transfer for the third step can be determined as follows:

$$\begin{aligned} \dot{Q} = &\left[n\left(\overline{h}_f^0+\overline{h}-\overline{h}^{0}\right)\right]_{CuCl_2}+\left[n\left(\overline{h}_f^0+\overline{h}-\overline{h}^{0}\right)\right]_{H_2} \\ &-\left[n\left(\overline{h}_f^0+\overline{h}-\overline{h}^{0}\right)\right]_{Cu}-\left[n\left(\overline{h}_f^0+\overline{h}-\overline{h}^{0}\right)\right]_{HCl}. \end{aligned} \tag{23}$$

The destroyed exergy is written:

$$\begin{aligned} Ex_{\text{dest}} = & \left[\left(\overline{h}-\overline{h}^{0}\right)-T_0\left(\overline{s}-\overline{s}^{0}\right)+\overline{ex}^{\,ch}\right]_{\text{Cu}} \\ & +\left[\left(\overline{h}-\overline{h}^{0}\right)-T_0\left(\overline{s}-\overline{s}^{0}\right)+\overline{ex}^{\,ch}\right]_{\text{HCl}} \\ & -\left[\left(\overline{h}-\overline{h}^{0}\right)-T_0\left(\overline{s}-\overline{s}^{0}\right)+\overline{ex}^{\,ch}\right]_{\text{CuCl}_2} \\ & -\left[\left(\overline{h}-\overline{h}^{0}\right)-T_0\left(\overline{s}-\overline{s}^{0}\right)+\overline{ex}^{\,ch}\right]_{\text{H}_2}+\left(1-\frac{T_0}{T_{\text{rea}}}\right)\dot{Q}. \end{aligned} \tag{24}$$

The energy and exergy analyses are done by using the first and second laws for the development of the heat transfer and the exergy destroyed as well as the exergy yield of each chemical reaction. Using the EES software leads to the following results described in the next section.

5 Results and discussion

5.1 First chemical reaction

Figure 6 presents the change of molar heat in terms of the reaction temperature. The amount of heat is given to the system by the surroundings. There is a linear decrease with the molar temperature due to the molar en-

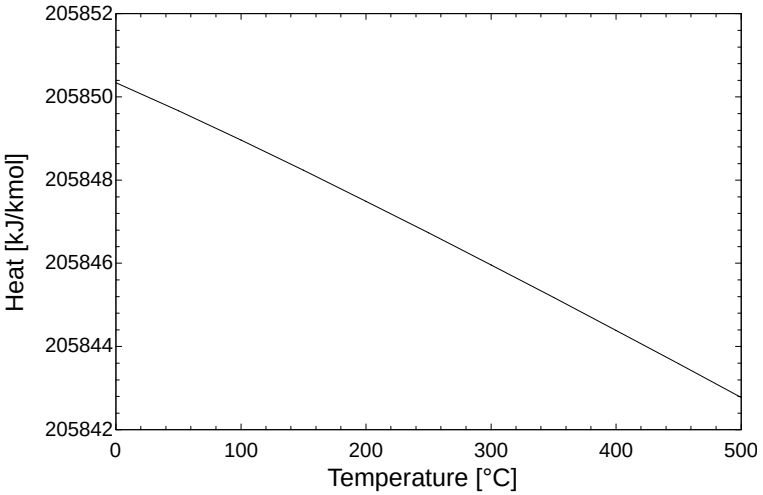

Figure 6: Variation of molar heat transfer with reaction temperature.

thalpy such as the enthalpy of standard formation ($\overline{h}_f^0$), sensible enthalpy ($\overline{h}$) and reaction enthalpy ($\overline{h}^0$). The enthalpy of copper chloride component is higher than the molar enthalpy of both copper and chlorine components. It is preferable to use high temperatures to save the thermal heat and improve thus the performance of the reaction. Results available in the literature show the same trends [22, 47].

Figure 7 shows that the destroyed exergy decreases non-linearly with increasing the reaction temperature. The exergy of products (copper exergy and chlorine) is higher than the exergy of reactants (copper-chlorine exergy). In contrast to energy, the exergy depends on both the surroundings and the system. That's why, and according to Eq. (9), the exergy is written as a function of ambient temperature T_0. This is the reason why we vary the surroundings temperature from –10°C in winter to 50°C in summer, corresponding to the maximum and minimum ambient temperature in Laghouat city, Algeria.

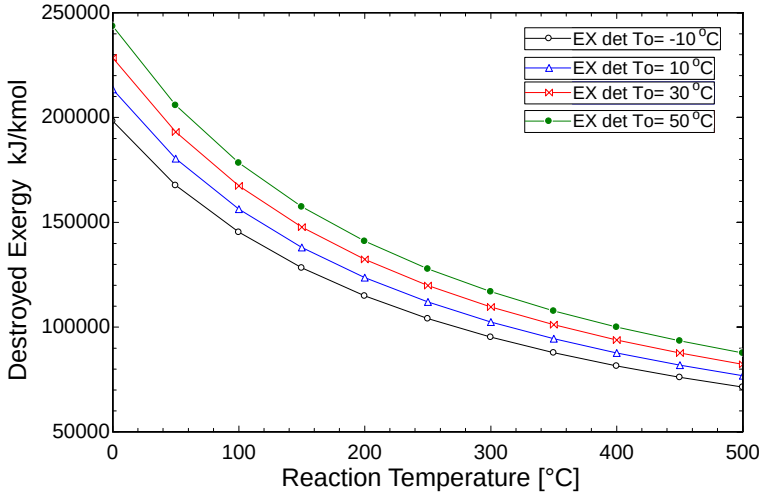

Figure 7: Variation of the destroyed exergy with the reaction temperature for several surrounding temperatures.

The exergy efficiency of the first step, Fig. 8, changes in the range 0.14–0.74 and increases with the increase of the reaction temperature. This is due to the exergy of products such as copper (Cu) and chlorine (Cl_2) being higher than the exergy of reactants (copper chloride, $CuCl_2$) since at high temperatures, the exergy is higher while the irreversibilities decrease, enhancing thereby the cycle performance.

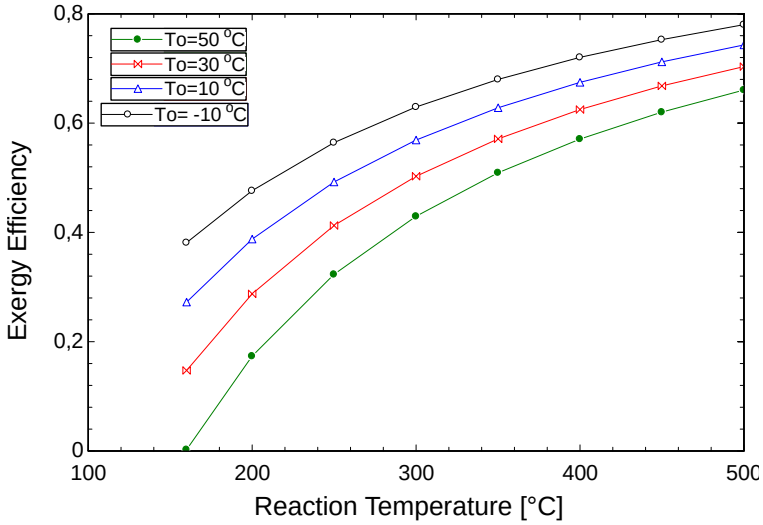

Figure 8: Variation of the exergy efficiency with the reaction temperature at several surrounding temperatures.

5.2 Second chemical reaction

Figure 9 shows a variation of the molar heat with the change in reaction temperature for the second reaction. In this reaction, the amount of molar heat transfer is provided by the surroundings to the system. As the reaction temperature rises, the amount of heat decreases due to the fact that the molar enthalpy of water and the gas chlorine are higher than the molar enthalpy of the hydrochloric acid and oxygen gas. It is recommended to use temperatures up to 300°C to save thermal energy and enhance the reaction performance.

Figure 10 shows that the exergy declines in a non-linear manner with the temperature of reaction and with increasing the surrounding temperature. This is because the exergy of the products (hydrochloric acid and oxygen) is higher than the exergy of the reactants, i.e. water and chlorine. Therefore, more exergy in the form of heat is obtained. Irreversibilities, such as chemical reactions and heat transfer always generate entropy and any transformation produced by entropy causes the destruction of exergy. Greater irreversibility during the process causes greater destruction of exergy.

Figure 11 shows the exergy efficiency of the second step, varying in the range from 0.1 to 0.48. Increasing the temperatures of the reaction and surroundings increases the exergy. This is due to the exergy of products,

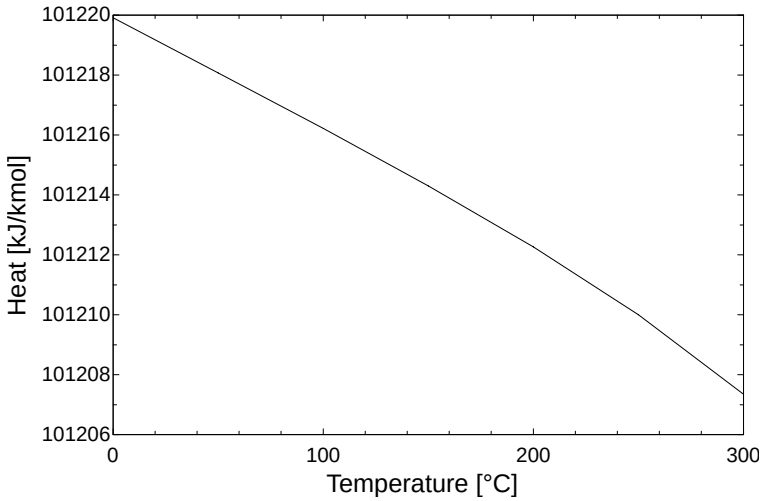

Figure 9: Variation of the molar heat transfer with reaction temperature.

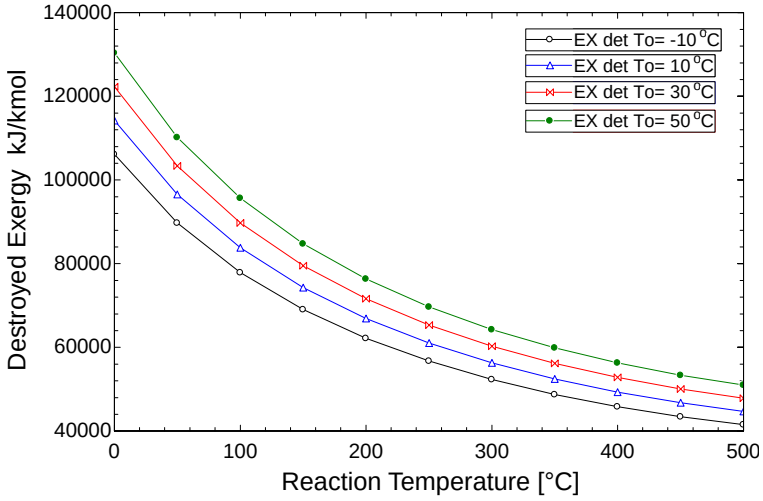

Figure 10: Variation of the destroyed exergy with the reaction temperature for several surrounding temperatures.

that is hydrochloric acid and oxygen, which is higher than the exergy of reactants (water and chlorine). At high temperatures, the exergy increases and the irreversibilities decrease. This leads to enhancement of the economic performance. It is noticed that the yield is almost non-existent at low temperatures whereas it grows rapidly at high temperatures.

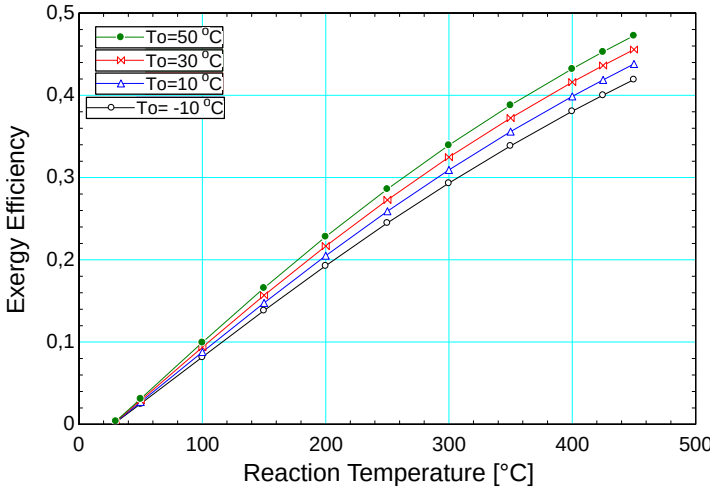

Figure 11: Variation of the exergy efficiency with the reaction temperature for different surrounding temperatures.

5.3 Third chemical reaction

Figure 12 depicts the change in molar heat with the temperature for the third step. As mentioned before, this reaction is the main interaction for the hydrogen production and the two previous steps are only for recycling the chemical elements. We take 0–100°C as the reaction temperature range.

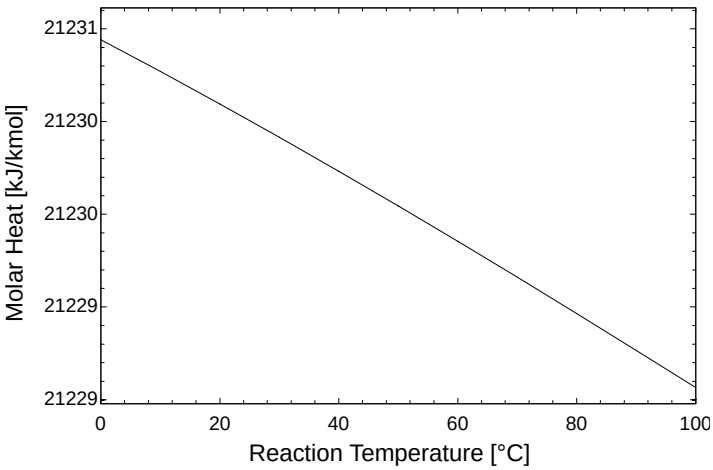

Figure 12: Variation of the molar heat transfer with the reaction temperature.

The amount of generated heat is rejected to the surroundings. The amount of heat produced by the reaction decreases slightly as the temperature of the reaction rises. In the closed range 0–100°C, the amount of heat may be expected to remain approximately constant. For this reason, it is preferable to work at ambient temperature 20–35°C to reduce the amount of heat provided and hence improve the performance of the cycle.

Figure 13 shows that the destroyed exergy increases non-linearly with increasing of the reaction temperature for different surroundings temperatures. This is due to the low exergy of products, ie. copper-chlorine and hydrogen when compared to the exergy of the reactants (copper and hydrochloric acid). One can observe that for the case of ambient temperature of 50°, the exergy is the lowest while at –10° the exergy is the largest for this step.

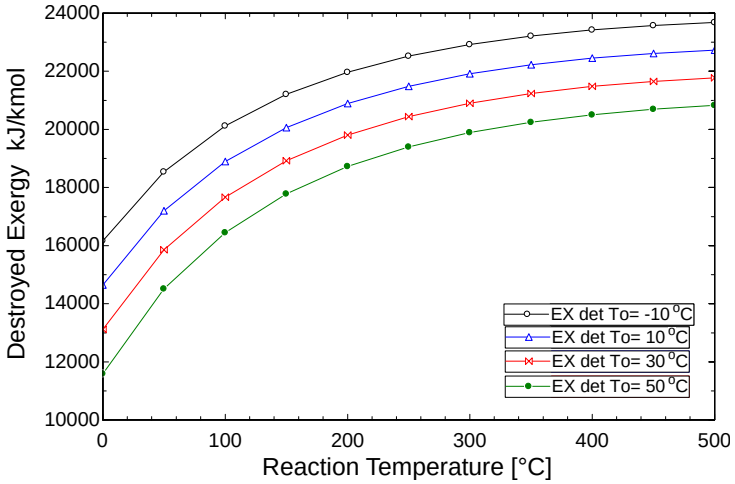

Figure 13: Destroyed exergy vs the reaction temperature for several surrounding temperatures.

The exergy efficiency of the third step, Fig. 14, changes from 0.72 to 0.98, with the external temperatures of –10, 10, 30°C and 50°C, respectively. It decreases with increasing the reaction temperature up to 140°C. This is explained by the exergy of products (hydrogen gas and copper chloride) which is higher than the exergy of the reactants such as copper and hydrochloric acid. At high temperatures the irreversibility increases and this is the main cause of degradation of the exergy efficiency. This confirms that this chemical reaction is viable at ambient temperatures.

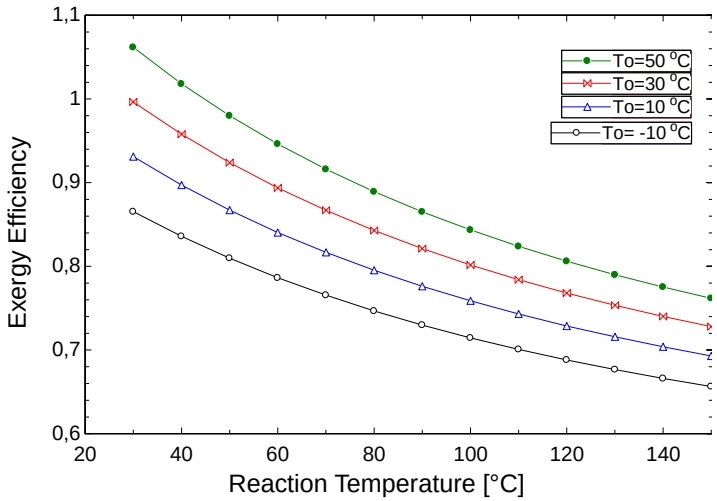

Figure 14: Variation of the exergy efficiency with the reaction temperature for different surrounding temperatures.

6 Overall exergetic yield

The exergetic yield of the chemical reactions is calculated without considering the heat losses. The product of exergetic yields of all chemical reactions is used to calculate the overall exergetic yield. The three steps in Table 5 are performed at $T_0 = 30°C$ and $P_0 = 1$ bar. The cycle's overall exergetic efficiency is determined by:

$$\eta_{ex\,\text{overall}} = \eta_{R1}\ \eta_{R2}\ \eta_{R3}\,. \tag{25}$$

The exergetic yield of each step is calculated as in Table 5, and the overall exergy efficiency of the cycle for hydrogen production is found to be 30.5%.

Table 5: Exergy yield of chemical reactions.

Step	Reactions	Q [kJ/kmol]	T_{rea} [°C]	T_0 [°C]	η_{ex} [%]
1	$CuCl_2(s) + Q \rightarrow Cu(s) + Cl_2(g)$	205844	500	30	0.624
2	$H_2O(l) + Cl_2(g) + Q \rightarrow 2HCl(g) + \frac{1}{2}O_2(g)$	101207	450	30	0.502
3	$2HCl(g) + Cu(s) \rightarrow CuCl_2(s) + H_2(g) + Q$	–21230	35	30	0.976

7 Conclusions

In this work, a new thermochemical cycle has been proposed for the production of hydrogen at relatively low temperatures. This cycle is based on chemical elements of copper-chlorine (Cu–Cl) for dissociating water molecules into hydrogen and oxygen. The process comprises three physical steps in the form of a closed internal boucle that continuously recycles all copper-chlorine molecules in which the products of the first reaction are the reactants of the following step and so on. The principal reaction is that related to hydrogen production, and the two remaining ones are used to recycle the chemical components for the continuity of the process. The study of the Gibbs function of the three chemical equations shows it to be negative, which means that the reactions are spontaneous and thus feasible, whereas the first law of thermodynamics allowed us to determine the molar heats of the equations, which are 205844 kJ/kmol, 101207 kJ/kmol and –21230 kJ/kmol (exothermic reaction), respectively. In addition, the appropriate temperature for each equation is determined where the heat calculated for the needs of reactions of the pure thermochemical cycle is a critical detail for the design of thermal sources. The highest temperature for this cycle is 500°C, which is relatively low when compared to other available cycles. The exergy efficiency of the three steps is found to be 62.4%, 50.2% and 97.6%, respectively, while the overall exergetic yield of the thermochemical cycle is 30.5%, which it is promising as compared to that of other different cycles. The current cycle mainly uses thermal energy that could be retrieved from the solar thermal field for the sustainability of the system.

The electro-thermochemical version can be proposed in future research to improve the efficiency of this cycle. In addition, a techno-economic study could be conducted to assess the feasibility of this process.

Acknowledgments

The authors gratefully acknowledge the Algerian Ministry of Higher Education and Scientific Research for their and facilities provided in the field of scientific research.

Received 20 September 2022

References

[1] Safari F., Dincer I.: *A review and comparative evaluation of thermochemical water splitting cycles for hydrogen production*. Energ. Convers. Manage. **205**(2019), 112182.

[2] Balta M.T.: *Thermodynamic performance assessment of boron based thermochemical water splitting cycle for renewable hydrogen production*. Int. J. Hydrogen Energ. **45**(2020), 60, 34579–34586.

[3] Rosen M.A.: *Advances in hydrogen production by thermochemical water decomposition: A review*. Energy **35**(2010), 2, 1068–1076.

[4] Dincer I.: *Green methods for hydrogen production*. Int. J. Hydrogen Energ. **37**(2012), 2, 1954–1971.

[5] Sattler C., Roeb M., Agrafiotis C., Thomey D.: *Solar hydrogen production via sulphur based thermochemical water-splitting*. Sol. Energy **156**(2017), 30–47.

[6] Pregger T., Graf D., Krewitt W., Sattler C., Roeb M., Möller S.: *Prospects of solar thermal hydrogen production processes*. Int. J. Hydrogen Energ. **34**(2009), 10, 4256–4267.

[7] Razi F., Dincer I., Gabriel K.: *Energy and exergy analyses of a new integrated thermochemical copper-chlorine cycle for hydrogen production*. Energy **205**(2020), 117985.

[8] Mao Y., et al.: *Hydrogen production via a two-step water splitting thermochemical cycle based on metal oxide – A review*. Appl. Energ. **267**(2020), 0360–0377.

[9] Farsi A., Dincer I., Naterer G.F.: *Multi-objective optimization of an experimental integrated thermochemical cycle of hydrogen production with an artificial neural network*. Int. J. Hydrogen Energ. **45**(2020), 46, 24355–24369.

[10] Bensenouci A., Medjelled A.: *Thermodynamic and efficiency analysis of solar steam power plant cycle*. Int. J. Renew. Energ. Res. **6**(2016), 4, 1556–1564.

[11] Naghavi S.S., He J., Wolverton C.: *$CeTi_2O_6$ – A promising oxide for solar thermochemical hydrogen production*. ACS Appl. Mater. Interface. **12**(2020), 19, 21521–21527.

[12] Hoskins A.L., et al.: *Continuous on-sun solar thermochemical hydrogen production via an isothermal redox cycle*. Appl. Energ. **249**(2019), 368–376.

[13] Dhif K., Mebarek-Oudina F., Chouf S., Vaidya H., Chamkha A.J.: *Thermal analysis of the solar collector cum storage system using a hybrid-nanofluids*. J. Nanofluids **10**(2021), 4, 616–626.

[14] Ju L.C.: *Energy optimization of a Sulfur-Iodine thermochemical nuclear hydrogen production cycle*. Nucl. Eng. Technol. **53**(2021), 2066–2073.

[15] Yildiz B., Kazimi M.S.: *Efficiency of hydrogen production systems using alternative nuclear energy technologies*. Int. J. Hydrogen Energ. **31**(2006), 77–92.

[16] Dou B., Zhang H., Song Y., Zhao L., Jiang B., He M.: *Sustainable energy & fuels hydrogen production from the thermochemical conversion of biomass*. Sustain. Energ. Fuels **3**(2019), 2, 314–342.

[17] Ghazvini M., Sadeghzadeh M., Hossein M.: *Geothermal energy use in hydrogen production: A review*. Int. J. Energ. Res. **10**(2019), 1–29.

[18] Temiz M., Dincer I.: *Concentrated solar driven thermochemical hydrogen production plant with thermal energy storage and geothermal systems*. Energy **219**(2021), 119554.

[19] Cui B., Zhang J., Liu S., Liu X., Zhang Z., Sun J.: *A low-temperature electrothermochemical water-splitting cycle for hydrogen production based on $LiFeO_2/Fe$ redox pair*. Int. J. Hydrogen Energ. **45**(2020), 41, 20800–20807.

[20] Qian X., et al.: *Article outstanding properties and performance of $CaTi_{0.5}Mn_{0.5}O_3$ for solar-driven thermochemical hydrogen production*. Matter **4**(2021), 2, 688–708.

[21] El-Emam R.S., Ozcan H., Zamfirescu C.: *Updates on promising thermochemical cycles for clean hydrogen production using nuclear energy*. J. Clean. Prod. **262**(2020), 121424.

[22] Abanades S., Charvin P., Flamant G., Neveu P.: *Screening of water-splitting thermochemical cycles potentially attractive for hydrogen production by concentrated solar energy*. Energy **31**(2006), 14, 2805–2822.

[23] Izanloo M., Mehrpooya M.: *Integrated thermochemical Mg-Cl-Na hydrogen production cycle, carbon dioxide capture, ammonia production, and methanation*. Int. J. Energ. Res. **10**(2021), 1–19.

[24] Safari F., Dincer I.: *A study on the Fe–Cl thermochemical water splitting cycle for hydrogen production*. Int. J. Hydrogen Energ. **45**(2020), 38, 18867–18875.

[25] Huang I., Zhang Y., Arafa M.: *High performance dual-electrolyte magnesium–iodine batteries that can harmlessly resorb in the environment or in the body*. Energ. Environ. Sci. **15**(2022), 10, 4095–4108.

[26] Balta M.T., Dincer I., Hepbasli A.: *ScienceDirect Comparative assessment of various chlorine family thermochemical cycles for hydrogen production*. Int. J. Hydrogen Energ. **41**(2016), 19, 7802–7813.

[27] Naterer G.F., Gabriel K., Wang Z.L., Daggupati V.N., Gravelsins R.: *Thermochemical hydrogen production with a copper-chlorine cycle. I: oxygen release from copper oxychloride decomposition*. Int. J. Hydrogen Energ. **33**(2008) 20, 5439–5450.

[28] Orhan M.F., Dincer I., Rosen M.A.: *An exergy–cost – energy–mass analysis of a hybrid copper-chlorine thermochemical cycle for hydrogen production*. Int. J. Hydrogen Energ. **35**(2010), 10, 4831–4838, 2010.

[29] Corgnale C., Ma Z., Shimpalee S.: *Modeling of a direct solar receiver reactor for decomposition of sulfuric acid in thermochemical hydrogen production cycles*. Int. J. Hydrogen Energ. **44**(2019), 50, 27237–27247.

[30] Farsi A., Dincer I., Naterer G.F.: *Second law analysis of $CuCl_2$ hydrolysis reaction in the Cu–Cl thermochemical cycle of hydrogen production*. Energy **202**(2020), 117721.

[31] Abdulrahman M.W.: *Simulation of materials used in the multiphase oxygen reactor of hydrogen production Cu–Cl cycle*. In: Proc. 6$^{\text{th}}$ Int. Conf. on Fluid Flow, Heat Mass Transf., FFHMT **123**(2019) 1–7.

[32] Khalid F., Dincer I., Rosen M.A.: *Thermodynamic viability of a new three step high temperature Cu–Cl cycle for hydrogen production.* Int. J. Hydrogen Energ. **43**(2018), 41, 18783–18789.

[33] Ozbilen A., Dincer I., Rosen M.A.: *A comparative life cycle analysis of hydrogen production via thermochemical water splitting using a Cu–Cl cycle.* Int. J. Hydrogen Energy, **36**(2011), 17, 11321–11327.

[34] Singh R.V., et al.: *Investigations on the hydrolysis step of copper-chlorine thermochemical cycle for hydrogen production.* Int. J. Energy Res., **44**(2020), 4, 2845–2863.

[35] Mebarek-Oudina F.: *Convective heat transfer of Titania nanofluids of different base fluids in cylindrical annulus with discrete heat source.* Heat Transfer – Asian Res. **48**(2019), 135–147.

[36] Dehghani S., Sayyaadi H..: *Energy and exergetic evaluations of Bunsen section of the sulfure iodine thermochemical hydrogen production plant.* Int. J. Hydrogen Energy, **38**(2013), 22, 9074–9084.

[37] EES Engineering Equation Solver Guide 2013. https://fchartsoftware.com/ees/ (accessed 13 Jan.2012)

[38] Hassan M., Mebarek-Oudina F., Faisal A., Ghafar A., Ismail A.I.: *Thermal energy and mass transport of shear thinning fluid under effects of low to high shear rate viscosity.* Int. J. Thermofluids **15**(2022), 100176.

[39] Bensenouci A., Teggar M., Medjelled A., Benchatti A.: *Thermodynamic analysis of hydrogen production by a thermochemical cycle based on magnesium-chlorine.* Int. J.Heat Technol. **39**(2021), 2, 521–530.

[40] Atkins P., De Paula J.: *Physical Chemistry for the Life Sciences.* Oxford Univ. Press, New York 2006.

[41] Stryer L.: *Biochemistry* Vol. 3. Freeman Comp., New York 1988.

[42] Al-Zareer M., Dincer I., Rosen M.A.: *Analysis and assessment of a hydrogen production plant consisting of coal gasification, thermochemical water decomposition and hydrogen compression systems.* Energy Convers. Manag. **157**(2017), 600–618.

[43] Canavesio C., Nassini D., Nassini H.E., Bohé A.E.: *Study on an original cobalt-chlorine thermochemical cycle for nuclear hydrogen production.* Int. J. Hydrogen Energy, **45**(2020), 49, 26090–26103.

[44] Yilmaz F., Balta M.T.: *ScienceDirect Energy and exergy analyses of hydrogen production step in boron based thermochemical cycle for hydrogen production.* Int. J. Hydrogen Energy **4**(2016), 1–7.

[45] Dincer I., Tolga M.: *Potential thermochemical and hybrid cycles for nuclear-based hydrogen production.* Int. J. Energy Res. **35**(2011), 123–137.

[46] Tolga M., Dincer I., Hepbasli A.: *Geothermal-based hydrogen production using thermochemical and hybrid cycles: A review and analysis.* Int. J. Energy Res. **34**(2010), 757–775.

[47] Orhan M.F., Dincer I., Rosen M.A.: *Energy and exergy assessments of the hydrogen production step of a copper-chlorine thermochemical water splitting cycle driven by nuclear-based heat.* Int. J. Hydrogen Energy **33**(2008), 22, 6456–6466.